ACS OMEGA

Article

Cite This: ACS Omega 2019, 4, 727−736

http://pubs.acs.org/journal/acsodf

Consequences of Heterogeneous Crowding on an Enzymatic Reaction: A Residence Time Monte Carlo Approach

Rajat Anand,[†,§] Manish Agrawal,[†,∥] Venkata Satish Kumar Mattaparthi,[†,⊥] Rajaram Swaminathan,[*,†] and Sitangshu Bikas Santra[‡]

[†]Department of Biosciences and Bioengineering and [‡]Department of Physics, Indian Institute of Technology Guwahati, Guwahati 781039, Assam, India

ABSTRACT: Translational diffusion of a free substrate in crowded metabolically active spaces such as cell cytoplasm or mitochondrial matrix is punctuated by collisions and nonspecific interactions with soluble/immobile macromolecules/macrostructures in a variety of shapes/sizes. It is not understood how such disruptions alter enzyme reaction kinetics in such spaces. A novel Monte Carlo (MC) technique, "residence time MC", has been developed to study the kinetics of a simple enzyme−substrate reaction in a crowded milieu using a single immobile enzyme in the midst of diffusing substrates and products. The reaction time lost while the substrate nonspecifically interacts or is transiently trapped with ambient macromolecules is quantified by introducing the residence time "tau". Tau scales with the size of crowding macromolecules but makes the knowledge of their shape redundant. The residence time thus presents a convenient parameter to realistically mimic the sticky surroundings encountered by a diffusing substrate in heterogeneously crowded physiological spaces. Results reveal that for identical substrate concentration and excluded volume, increase in tau significantly diminished enzymatic product yield and reaction rate, slowed down substrate/product diffusion, and prolonged their relaxation times. A smooth transition from the anomalous subdiffusive motion to normal diffusion at long time limits was observed irrespective of the value of tau. The predictions from the model are shown to be in qualitative agreement with in vitro experimental data revealing the rate of alkaline phosphatase-catalyzed hydrolysis of *p*-nitrophenyl phosphate in the midst of 40/500/2000 kDa dextrans. Our findings from the residence time MC model also attempt to rationalize previously unexplained experimental observations in crowded enzyme kinetics literature. Furthermore, major insights to emerge from this study are the reasons why free diffusion of the substrate in crowded physiological spaces is detrimental to enzyme function. It is argued that organized enzyme clusters such as "metabolon" may perhaps exist to regulate the substrate translocation in such sticky physiological spaces to maintain optimal enzyme function. In summary, this work provides key insights explaining why absence of substrate channeling can dramatically slow down enzyme reaction rate in crowded metabolically active spaces.

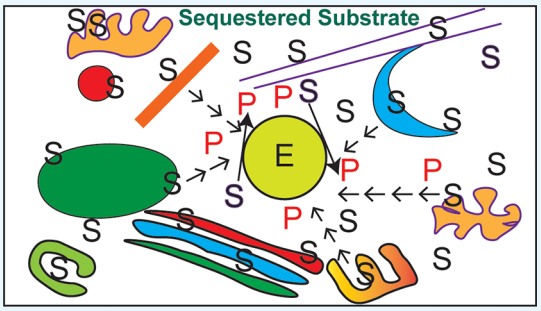

1. INTRODUCTION

Crowding by biomacromolecules, such as nucleic acids, proteins, and membranes, is an all pervasive phenomenon in intracellular milieu's such as cell cytoplasm (site for glycolysis),[1−4] mitochondrial matrix (site for tricarboxylic acid cycle),[5,6] and red blood cell interiors.[7] Recent reports suggest that cytoplasm of a prokaryotic cell may not be uniformly crowded but possess supercrowded multiplexes along with relatively uncrowded reservoirs.[8] Biochemical reaction kinetics in an intracellular environment can be fundamentally different from a test tube where reactants are dilute and perfectly mixed. It has been argued that in a nonhomogeneous crowded milieu, the law of mass action can break down and reactions may follow fractal-like kinetics.[9−11]

Diffusion enables substrates find their target enzyme active site within the limited dimensions of the animal cell (∼15 μm). Diffusion of a substrate in the intracellular milieu can be slowed by nonspecific (soft) interactions with crowding macromolecules and higher ambient microviscosity. Fluorescence recovery after photobleaching results of a fluorescent probe in cytoplasm[12−14] and mitochondrial matrix[5] have shown that this slowing occurs chiefly due to frequent collisions of the small molecule (probe) with cell solids which comprise 13−15% of isosmotic cell volume.[12] Such collisional encounters may transiently trap an intermediate/substrate of a metabolic pathway and slow down the metabolism. Measuring metabolite levels inside living cells has proved to be a challenging experimental task in itself.[15−19] It has been shown that molar concentration of an enzyme active site exceeds free substrate concentration in glycolytic pathways of rat or rabbit muscle,[20] hinting that free substrate cannot meet urgent metabolic demands. Measured diffusion coefficients of metabolites such as ATP inside the skeletal muscle[21] or rat cardiomyocytes[22] are 1.4−3.5 times slower

Received: October 18, 2018
Accepted: December 26, 2018
Published: January 9, 2019

DOI: 10.1021/acsomega.8b02863
ACS Omega 2019, 4, 727−736

compared to aqueous solutions, perhaps partly owing to gluey surroundings. Transient binding and unbinding of a protein to a fixed anchor in the membrane has been shown to lead to anomalous diffusion.[23] Binding of sequential enzymes in the glycolytic pathway to filaments has also been investigated.[24] Given that all 10 enzymes in the glycolysis pathway are in the cytosol,[25] the likelihood of a metabolite intermediate getting transiently entrapped in the crowded cytosol is a distinct possibility.

It is hence important to create a model to investigate how such soft interactions of the substrate (metabolite) with surrounding macromolecules (crowders or obstacles) influences the kinetics of an enzymatic reaction? For this purpose, the vast heterogeneity in shapes and sizes among the crowders in the cell interior must be accounted. Faithful representation of such morphological diversity among crowding macromolecules (Figure 1) in a lattice model can be tedious. Past attempts include assigning square[26] or cubic spaces[27] in the lattice, but these fall short in reproducing the sheer variety in crowder shapes. Here in this work, we attempt to address this challenge by modeling the nonspecific interaction of a substrate with an immobile crowding obstacle in a novel way that quantifies the interaction time, while making the shape of the crowder redundant.

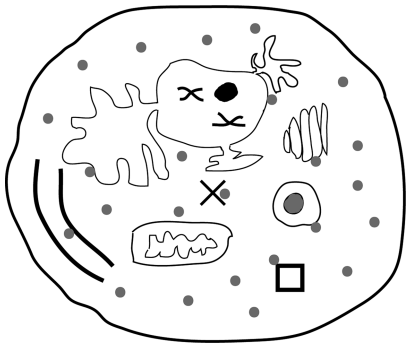

Figure 1. The Crowded Cell. The diversity in shapes and sizes of obstacles encountered by a substrate (filled grey circles) in a crowded cell cytoplasm is illustrated schematically (not to scale). The enzyme is represented by a cross in the center.

A tiny solute or substrate (~500 Da) in a crowded space such as cell cytoplasm encounters myriad barriers of an assortment of shapes and sizes (Figure 1) in its diffusive path. The translational diffusion of this substrate in such a milieu is hindered by three main factors.[12] These are: (a) crowding by large macromolecules or immobile structures that effectively reduce the available volume in the medium. As a result, the substrate encounters frequent collisions in its path, occasionally getting trapped locally within or between barriers; (b) binding transiently to obstacles in the medium; and (c) higher fluid-phase viscosity in the medium. Experiments have shown that factors (a) and (b) are the chief determinants for retarding solute translation in the cell cytoplasm. The complex interactions of a substrate or product with a macromolecule that include ballistic collisions, trapping, and transient binding are expected to scale up with macromolecular size. As the size of a macromolecule increases so does its exposed surface area available for the interaction with the substrate. The time spent by a substrate on the surface or accessible interior of the macromolecule is expected to rise with the macromolecule size because of transient but frequent substrate−macromolecule interactions aside from the strength of binding, which is likely to be weak and uniform. The diffusion of a substrate in a crowded milieu is therefore slowed down by two factors: (a) population density of the macromolecules (accounted by area fraction in a 2D lattice) and (b) size of the macromolecule with which it is interacting. In a dynamical process, such slowing down can be accounted for by introducing interaction time or residence time, τ. The residence time approach clearly decouples excluded volume effects from the size of the crowder. The former is now solely accounted by the population density of the crowder. It is thus intriguing to investigate the enzyme kinetics in a crowded milieu as a function of size and concentration of crowding macromolecules.

Several workers have in the past tried to model enzyme reactions in crowded media using Monte Carlo (MC) approaches in both two[9,28,29] and three dimensions.[26,30] To the best of our knowledge, residence time MC approach has not been applied by any so far. We believe that residence time is a realistic mimic of the unproductive encounters suffered by the substrate in a crowded cellular interior before it undergoes reaction.

In this paper, an approach based on nonequilibrium dynamics of enzymatic reactions in the diffusion-limited regime is considered. The objective is to understand qualitatively the influence of crowding by macromolecules of several different sizes on the rate of diffusion-limited enzymatic reactions governed by nonequilibrium thermodynamics. A simple numerical model in two dimensions (2D) based on molecular diffusion in disordered systems coupled with enzymatic reaction is proposed here. It is predicted that the rate of a diffusion-limited enzyme-catalyzed reaction will experience a monotonic decrease with increase in the fractional volume occupancy of the crowding agent and with the residence time that reflects the molecular size of the crowding obstacle. Subsequently, the results from the numerical model are compared with experimental findings obtained by measuring the enzymatic rate of alkaline phosphate-catalyzed hydrolysis of *p*-nitrophenyl phosphate (PNPP) in an aqueous medium crowded with dextran of molecular weight: 40, 500, or 2000 kDa present in a range of concentrations from 0 to 20% w/w. These predictions are shown to be in qualitative agreement with experimental observations carried out in vitro. Furthermore, our model is taken up to explain previous experimental results in literature. The implications of our model in understanding substrate diffusion inside crowded metabolically active spaces are discussed.

2. RESULTS AND DISCUSSION

2.1. Alkaline Phosphatase-Catalyzed Hydrolysis in a Crowded Medium. Experimentally measured initial reaction rates for alkaline phosphatase (enzyme, homodimer mol wt ~160 kDa)-catalyzed hydrolysis of *p*-nitrophenyl phosphate (substrate, mol wt 220 Da) in the presence of increasing dextran (40, 500, and 2000 kDa) size are presented here. This enzyme−substrate pair was chosen because (A) enhancement of enzymatic rate arising from increase in thermodynamic activity of alkaline phosphatase from dextran crowding is negligible as shown previously by our lab[31] and (B) size of the homodimeric enzyme is large enough (>140 kDa) to be sensitive to crowding by larger dextrans (>400 kDa) based on the discussion presented later. The 2000 kDa dextran was specifically chosen to bring out the role of increased

DOI: 10.1021/acsomega.8b02863
ACS Omega 2019, 4, 727−736

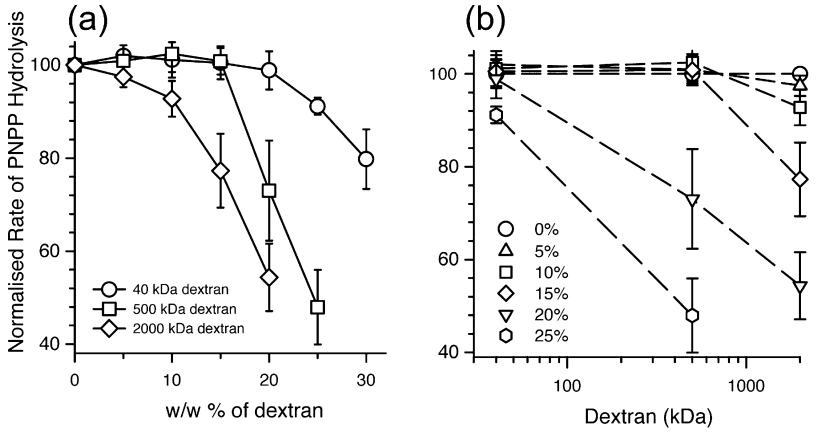

Figure 2. Rate of alkaline phosphatase-catalyzed hydrolysis in the presence of dextrans of different sizes. (a) Plot of average normalized reaction rate of alkaline phosphatase-catalyzed hydrolysis of *p*-nitrophenyl phosphate in the presence of dextrans of different sizes (40, 500, and 2000 kDa) against dextran concentration (in % w/w). (b) Plot of the same normalized rate against dextran molecular weight (proportional to residence time in the model) for different dextran concentrations.

nonspecific binding of the substrate to the dextran. This will enable comparison of the results with the model to be presented later.

Figure 2a shows gradual decrease in the reaction rate with increasing volume fraction (proportional to % w/w) of 40 kDa dextran. As the molecular size of dextran increases to 500 kDa, the decline in enzymatic rate appears more pronounced especially for higher volume fractions (20 and 25% w/w). This trend continues further for 2000 kDa dextran, where the rate drops to ∼50% at 20% w/w of this dextran size. Figure 2b shows a plot of Figure 2a data as a function of dextran size for different volume fractions. It is observed that significant slowing of reaction occurs only at high volume fractions (20 and 25% w/w) of 40 and 500 kDa dextrans. However, in presence of the largest dextran employed (2000 kDa), the slowing of reaction rate appears noticeable from 5% w/w itself. Further increase in volume fraction of this dextran (10−20% w/w) has a marked effect in slowing down the enzymatic reaction. Intriguingly, although the presence of 15% w/w of 500 kDa dextran had no measurable effect on the reaction rate, the presence of 2000 kDa at the same volume fraction slowed down the reaction by ∼20%. Such a dip in the rate cannot be accounted by excluded volume effects alone, especially as no measurable change was observed for the same volume fraction between 40 and 500 kDa dextran. Previous results[31] have demonstrated that conventional Michaelis−Menten kinetics is not applicable in a crowded medium which is far from ideal, where mixing is not uniform, law of mass action can break down, and rate constants can be time dependent.[9,10] For this reason, measurements of enzyme kinetic parameters were not pursued.

2.2. Questions Posed by Experimental Data.

(a) Results from Figure 2a reveal that at a constant volume fraction of 15%, crowding by 2000 kDa dextran exerts a marked decrease in catalytic activity in contrast to that by 40 or 500 kDa. Specifically, such effects appear more pronounced when size and density of the crowder is large. How can this be explained?

(b) Pastor et al. have studied the effect of crowding dextrans in a variety of sizes on the reaction rate of three different enzymes.[32] They showed that smaller enzymes (<42 kDa) showed no change in reaction rate when dextran size was raised from 50 to 150 kDa. However, with larger enzymes (∼140 kDa), reaction velocity decreases with the increasing dextran size (50−410 kDa) when higher concentrations of dextran (>50 mg/mL) are employed. How does enzyme size modulate the effects of dextran crowding on reaction kinetics?

(c) As described in the Introduction, it is not clear why are free glycolytic metabolites so scarce to find in rat/rabbit muscle?

(d) Why is the diffusion coefficient of ATP inside skeletal muscle and rat cardiomyocytes slowed down by 1.5−3.4 fold?

To seek answers to the above questions, we put forward the residence time MC model described below. We chose a 2D model to keep things simple.

2.3. The Model. At any instance of time, *t*, the system is composed of substrates S, an enzyme E, macromolecules (or obstacles) O, and products P. The spatial positions of E and O are kept fixed throughout the simulation. It is assumed that S and P both interact with the macromolecules O. But O, which are inert, neither interact with the enzyme E nor influence the enzymatic reaction directly. Diffusion of S and P in the system is modeled by random walk. During diffusion, every interaction of S with the enzyme E leads to immediate conversion of S to P. If S or P collide with an obstacle O, they interact with O for a while and are subsequently released. Hence, the above process of the enzymatic reaction can be represented as

$$\mathrm{S} + \mathrm{O} \rightarrow \mathrm{OS} \rightarrow \mathrm{O} + \mathrm{S}; \qquad \mathrm{S} + \mathrm{E} \rightarrow \mathrm{E} + \mathrm{P};$$
$$\mathrm{P} + \mathrm{O} \rightarrow \mathrm{OP} \rightarrow \mathrm{O} + \mathrm{P} \qquad (1)$$

where OS and OP represent the interacting states of S and P with O, respectively. The lifetimes of OS and OP are proportional to the size of the macromolecule and represented by the parameter called "residence time", τ. For simplicity, the residence time of OS and OP are assumed to be the same. Note that, the equilibrium Michaelis−Menten reaction reduces here to an irreversible one by instantaneous conversion of S to P. The final equilibrium state corresponds to conversion of all S to P. The model without incorporation of the residence time, τ, has been explained previously.[29]

A residence time MC algorithm is developed to study diffusion-limited enzymatic reactions given in eq 1 taking concentration and size of the macromolecules as parameters.

DOI: 10.1021/acsomega.8b02863
ACS Omega 2019, 4, 727−736

The algorithm is developed on a square lattice of size $L \times L$ defined on the xy-plane in 2 dimensions (2D). All elements, S, P, O, and E are represented as point particles in this model. As the interaction of S and P with a macromolecule is proportional to its size, the size of a macromolecule in this model is taken care in terms of the interaction time of S or P with O and is represented by the size dependent residence time, τ. The size of the enzyme is reduced to a point particle just to reduce the complexity of the problem. The single enzyme is placed at the center of the lattice, and S and O are distributed randomly over the rest of the lattice sites with their respective concentrations, C_S and C_O. A lattice site is either empty or occupied by any one of the elements. As E and O remain immobile throughout the simulation, the diffusion of S and P in the crowded milieu is studied in the following manner. Depending on the status of the destination site, there are four possibilities: (a) if the destination site is empty, S or P moves to the destination site from the present site, (b) if the destination site is occupied by another S or P, they remain on the same site and no displacement occurs, (c) if the destination site is occupied by an O, P or S remains on the same site for τ MC time steps, and (d) if the destination site is occupied by the enzyme E, P remains on the same site but S is converted to P with unit probability. The interaction time between the enzyme and the product is neglected in this model. As soon as all S and P are checked for an attempt of motion, time, t (the MC time step), is increased to $t + 1$. The maximum area fraction, $a_f = C_S + C_O$ taken is 0.4, far below the percolation threshold of ≈0.59 for the site percolation on the square lattice.[33] Cyclic boundary condition has been applied for the motion of S and P in both x and y directions. Reaction kinetics is monitored by keeping track of population of products formed and the average diffusion length of product molecules from the center of the lattice as a function of MC time steps.

System morphology for three different values of $\tau = 0$, 2, and 8 at MC step, $t = 2^{12}$, 2^{18}, and 2^{20} are shown in Figure 3 for a system with $a_f = 0.1$ and $C_S = 0.01$. It can be seen that the substrates (black dots) are converted to products (gray squares) and are uniformly distributed over the lattice. For $\tau = 0$, the macromolecules are simple obstacles and correspond to hindrance to diffusion. The conversion rates decrease significantly with increasing residence time, τ, as there are more and more unreacted substrates left for higher values of τ. Interestingly, at $t = 2^{20}$, although there are no substrates in the immediate vicinity of the enzyme for $\tau = 0$ and 2, a significant substrate population in close vicinity of the enzyme is observed for $\tau = 8$.

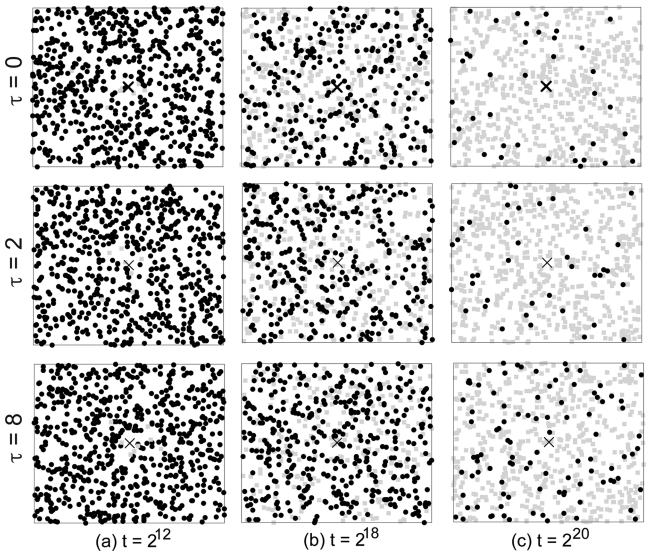

Figure 3. The model. System morphology at MC step (a) $t = 2^{12}$; (b) $t = 2^{18}$; and (c) $t = 2^{20}$ for three different values of $\tau = 0$ (top), 2 (middle), and 8 (bottom) is shown with $a_f = 0.1$ and $C_S = 0.01$. The black dots represent the substrate S and the gray squares represent the product P. The single enzyme is shown by a cross at the center of the lattice. For clarity, obstacles are not shown.

To have a qualitative explanation of the experimental results, estimates of initial reaction rates, diffusivity, and system relaxation are made below for different parameter sets.

2.4. Results Obtained Using the Model. Simulations were carried out for 2^{20} (a little more than a million) MC time steps on a 256×256 square lattice. The data are averaged over 100 ensembles. There are two parameters in the system, the crowder concentration, (C_O), and residence time, τ (macromolecular size). The system is studied for different area fractions, $a_f = C_S + C_O$, and for different residence times, τ, for a given C_S to observe the effect of crowder concentration and that of the size of the macromolecules on the yield of the enzymatic reaction. The enzymatic reactions are characterized mainly by calculating reaction rates and diffusivity of the system.

2.4.1. Reaction Rate. To calculate the kinetic reaction rate, the number of products, $N_P(t)$, is recorded with time, t, the MC time step for a given area fraction a_f, and residence time, τ. At any instant of time, the total number of molecules, that is the number of substrate and product molecules, in the system is conserved and is given by $N_S(t) + N_P(t) = N_S(0)$, where $N_S(0) = C_S \times L^2$ is the number of substrate molecules initially given. As per equilibrium reaction kinetics, it is expected that the total number of products, $N_P(t)$, at any time, t, is given by

$$N_P(t) = N_S(0)(1 - e^{-\alpha t}) \quad (2)$$

where α is the reaction rate constant. To study the effect of a_f and τ on the time evolution of the yield, the relative yields, $N_P(t)/N_S(0)$, are plotted against time, t, for different values of a_f, for fixed $C_S = 0.01$, and $\tau = 0$ in Figure 4a and for different values of τ for fixed $a_f = 0.1$ and $C_S = 0.01$ in Figure 4b. The yield, N_P, increases slowly initially, followed by a rapid increase, and finally saturates in the long time limit irrespective of the parameter values. For low a_f or small τ, it can be seen that the reaction is almost complete, that is, substrates given initially are fully converted to products. However, there is a considerable decrease in the product yield with increase in a_f and with increase in τ. With higher values of τ and a_f, the reactions appear slow and remain incomplete after $t = 10^6$ MC steps. It has been predicted by numerical simulations that classical Michaelis–Menten kinetics may not apply to enzymatic reactions in crowded media.[9] In a 1D model of reaction diffusion with disorder, Doussal and Monthus[34] also found large time decay in the species density via real space renormalization group calculations. As most molecular processes are characterized by the initial rate of an enzymatic reaction, it is estimated keeping only the linear term of the exponential series in eq 2. To collect data in the linear regime of the reaction kinetics, the yield is calculated after 20% conversion of the substrates to products for a given parameter set. The effects of area fraction, a_f, and residence time, τ, on the reaction rates are shown in the insets of Figure 4a,b,

DOI: 10.1021/acsomega.8b02863
ACS Omega 2019, 4, 727−736

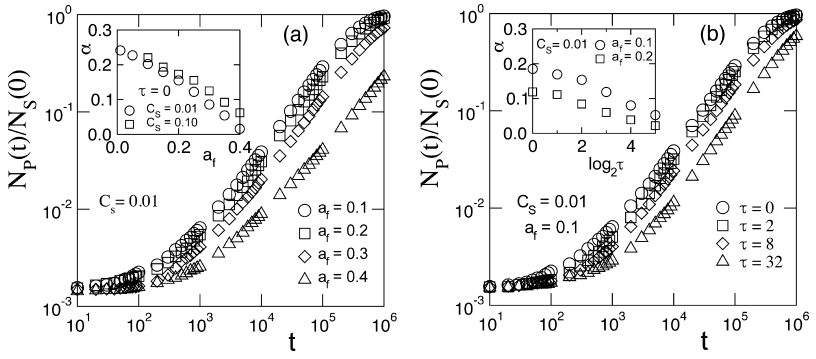

Figure 4. Crowding and product yield of the reaction. Plot of $N_P(t)/N_S(0)$ vs time t, (a) for different area fractions, $a_f = C_S + C_O$, keeping $C_S = 0.01$ and $\tau = 0$ and (b) for different residence time, τ, keeping $C_S = 0.01$, $a_f = 0.1$. Variation of the reaction rate, α, against a_f for $C_S = 0.01$ (circles) and 0.1 (squares) with $\tau = 0$ is shown in the inset of (a), whereas the same against τ for $a_f = 0.1$ (circles) and 0.2 (squares) with $C_S = 0.01$ is displayed in the inset of (b).

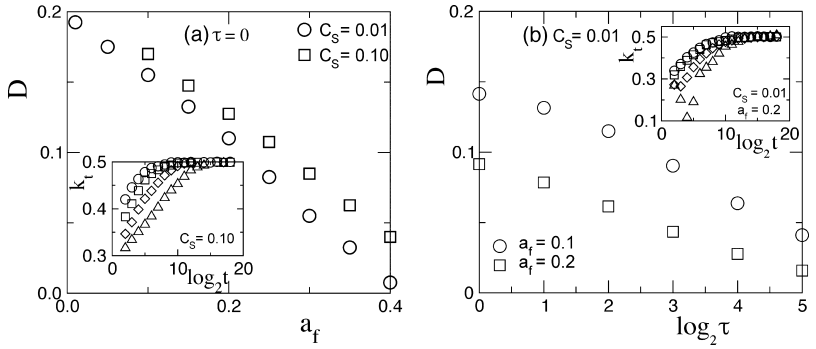

Figure 5. Crowding, residence time, and diffusion. (a) Plot of D against a_f for $C_S = 0.01$ (circles) and 0.10 (squares) with $\tau = 0$. (b) Plot of D against τ for $a_f = 0.1$ (circles) and 0.2 (squares) with $C_S = 0.01$. In the inset of (a), k_t is plotted against $\log_2 t$ for several values of a_f (legend symbols correspond to the same values of a_f as shown in Figure 4a) with $C_S = 0.10$ and $\tau = 0$; whereas the same are plotted for several values of τ (legend symbols correspond to the same values of τ as shown in Figure 4b) with $a_f = 0.2$ and $C_S = 0.01$ in inset of (b).

respectively. For $\tau = 0$, the effect of area fraction, a_f, on α is studied for two different substrate concentrations, $C_S = 0.01$ and $C_S = 0.10$. There are a few things to notice. First, α is decreasing with the increase in area fraction, a_f, for a given C_S in a nonlinear fashion as it is observed in experiments.[35−37] Note that the thermodynamic effect of crowding on enzyme activity is neglected here. As a consequence, the observed dependence of the reaction rate on crowder concentration is different from the prediction made by Ellis.[38] Second, at any given area fraction, a_f, there is a subtle increase in α with the increase in C_S due to the increased likelihood of enzyme−substrate encounter at a higher C_S. Third, α is approaching zero as the area fraction, a_f, approaches $1 - p_c \approx 0.4$, where $p_c \approx 0.59$ is the percolation threshold on a square lattice.[33] For $a_f > 0.4$, the spanning path of the empty sites may get blocked as the concentration of empty sites would become less than 60%. Consequently, the substrate molecules are trapped within the dangling ends of the clusters formed by the obstacles and unable to encounter the enzyme. As a result, α is expected to decrease and go to zero at high area fraction. The effect of macromolecular obstacle size on the reaction rate, α, is another important aspect to look into. As the obstacle size is represented by τ, the variation of the reaction rate, α, against τ for two different area fractions, $a_f = 0.1$ and $a_f = 0.2$, for a given substrate concentration, $C_S = 0.01$ are shown in the inset of Figure 4b. The reaction rate drops substantially as τ becomes nonzero and decreases further as τ increases. In fact, $\alpha \approx 0$ at $\tau = 32$. The drop in α in this case is because of the fact that, for a fixed a_f, as τ increases, the interactions of S and P with O increase and both of them remain immobile for some time that is proportional to τ. As a result, the substrate enzyme interaction becomes less frequent and the product yield decreases. This event captures qualitatively the situation where the substrate molecules are trapped or bound to a macromolecule for longer and longer periods. It can also be noticed that for a given τ, α is less for $a_f = 0.2$ compared to $a_f = 0.1$. This difference diminishes with increase in τ. As τ increases, the effect of τ predominates over the effect of crowding exerted by the higher area fraction. a_f.

$$\alpha = \lim_{t\to 0} \frac{1}{t} \frac{N_P(t)}{N_S(0)} \tag{3}$$

2.4.2. Diffusivity. Enzyme reaction inside a cell cytoplasm involves several steps, namely, (i) diffusion of a large number of substrate molecules through the complex milieu of inert macromolecules, (ii) reaction of substrate with the enzyme to yield products, and (iii) finally, diffusion of products away from the enzyme (sometimes as target substrate for the next enzyme in the pathway) through the same complex milieu of macromolecular crowding. The diffusion process occurring here involves the collective motion of a large number of particles in presence of disorder, which is a more complex process than diffusion of a single tracer particle in a disordered medium. The macromolecules surrounding the E, S, or P are inert in the sense that they do not influence the enzymatic reaction. However, the inert macromolecules could trap S or P

DOI: 10.1021/acsomega.8b02863
ACS Omega 2019, 4, 727−736

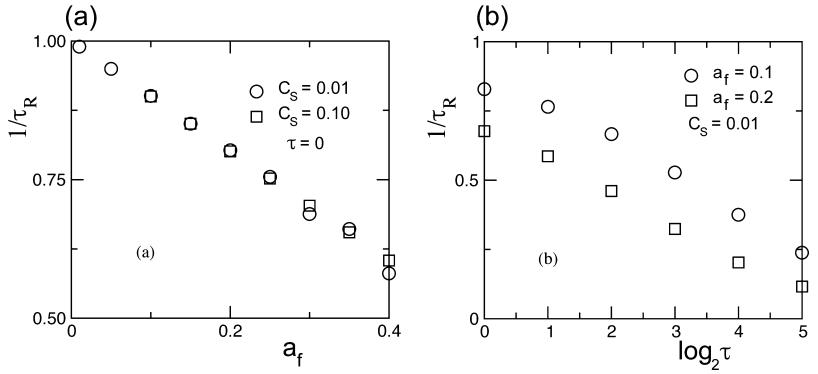

Figure 6. Crowding and relaxation time. (a) Plot of $1/\tau_R$ against a_f for $C_S = 0.01$ (circles) and 0.10 (squares) with $\tau = 0$. (b) Plot of $1/\tau_R$ against τ for $a_f = 0.1$ (circles) and 0.2 (squares) with $C_S = 0.01$.

when they come in contact during diffusion. In that sense, they are "active" disorder and one needs to study the diffusion of S or P in presence of such "active" disorder. Generally, diffusion is modeled by random walk, and the disordered system is modeled by spanning percolation clusters.[33] For studying diffusion, a quantity of interest is the root mean square (rms) distance, $r(t)$, covered by the diffusing particle in time, t. The rms distance, $r(t)$, in 2D is given by

$$r^2(t) = 4D \times t^{2k} \tag{4}$$

where D is the diffusivity of the system and k is an exponent which has a value 1/2 for diffusion on a regular lattice. On the percolation cluster, diffusion is found to be anomalous and the value of k becomes less than 1/2.[39,40] To check whether the enzyme kinetic reaction considered here is diffusion limited or not, the rms distance, $r(t)$, traveled by the product P after its birth in the vicinity of the enzyme is recorded in time, t. The data is then sample averaged over 100 ensembles. To analyze the diffusive behavior of the system, the local exponent, k_t, and the diffusivity, D, are estimated using eq 5.

$$k_t = \frac{1}{2}\frac{\mathrm{d}\ln r^2(t)}{\mathrm{d}\ln t} \text{ and } D = \lim_{t\to\infty}\frac{1}{4}\frac{\mathrm{d}r^2(t)}{\mathrm{d}t} \tag{5}$$

The effect of area fraction, a_f, and the residence time, τ, on k_t and D is studied. For $\tau = 0$, D is plotted against a_f for $C_S = 0.01$ and $C_S = 0.10$ in Figure 5a and for $a_f = 0.1$ and 0.2 with $C_S = 0.01$, it is plotted against τ in Figure 5b. Variations of k_t with time, t, for these parameters are shown in the inset of the respective figures. The diffusivity, D, is found to decrease with both a_f and τ. At the same time, it is important to notice that the exponent, k_t, approaches to a value 1/2 in the limit $t \to \infty$, irrespective of the values of a_f and τ. This is because at the start of the reaction, the system is not at equilibrium. As time progresses, the dynamic events make the system evolve and find its way. This enables diffusion to take shape and dominate. However, in a previous study,[30] certain anomalous behavior of k_t was observed in the case of low substrate concentration, $C_S = 0.01$, but high area fraction, $a_f = 0.4$, with $\tau = 0$. Such effect could arise if the products get trapped in a localized region without any connectivity path of empty sites. Saxton has shown that diffusion becomes more anomalous when obstacle concentration approaches percolation threshold.[41] In the long time limit, the process is then diffusive. It is interesting to note that the decrease in D with the increase in a_f or τ is in accordance with the decrease of the reaction rate, α, with the increase of the respective parameters (Figure 4, inset). The enzymatic reaction rate in these parameter regimes is therefore mostly governed by diffusion and can be considered a purely diffusion-limited enzymatic reaction. For a given area fraction, a_f, as the substrate concentration, C_S, is increased the diffusivity, D, is also marginally higher. Such increase in D is due to the fact that at higher C_S, the immobile obstacle concentration is less for a given a_f. Hence, the products have more free space to diffuse. On the other hand, for a fixed value of τ and C_S, if a_f is increased, D is decreased due to macromolecular crowding. It is more important to note that for a given C_S and a_f, if τ is increased, the diffusivity is found to decrease due to enhanced macromolecule−product (or substrate) interaction. Therefore, with the same C_S and a_f, crowding macromolecules with higher residence time affect the diffusivity and the enzymatic reaction rate more compared to those with lower residence time. Thus, increased stickiness of the crowder can profoundly diminish substrate diffusion and consequently the enzymatic reaction rate.

2.4.3. Relaxation Time. The decrease in diffusivity and the enzymatic reaction rate can also be understood in terms of relaxation time, τ_R. It is defined as the average time required to make a single move during the random walk of t MC time steps. The relaxation time, τ_R, is defined as

$$\tau_R = \frac{1}{N_S(0)}\sum_{j=1}^{N_S(0)}\frac{T_j}{N_m(j)} \tag{6}$$

where $N_m(j)$ is the number of moves made by the jth product (or substrate) during the period of random walk of T_j MC steps, that is the total number of attempts a random walker made during the walk and averaged over total number of diffusing particles, $N_S(0)$. Either due to absence/presence of crowding or due to the absence/presence of residence time, the product (or the substrate) can/cannot make a move to a nearest neighboring position in each and every MC time step. The relaxation time, τ_R, is then a measure of the average time taken to make a single move. In Figure 6, $1/\tau_R$ is plotted against a_f in (a) and against τ in (b). It can be seen that the inverse relaxation time, $1/\tau_R$, is decreasing (or the relaxation time is increasing) with increasing a_f or τ. From Figure 6a, it is evident that C_S has a little effect on the relaxation of the system. On the other hand, area fraction, a_f, and the residence time, τ, has a strong effect on the relaxation of the system. Because the relaxation time of the system is increasing with a_f and τ, the diffusivity of the system has to decrease and as a consequence the enzymatic reaction rate would be diminished.

DOI: 10.1021/acsomega.8b02863
ACS Omega 2019, 4, 727−736

In both Figures 5b and 6b, it is interesting to observe that rate of decrease in D and $1/\tau_R$ is reduced at low a_f (∼0.1) and moderate τ (1−2). This mild enhancement of diffusion in the presence of attractive crowders has been predicted before.[42] We now compare results obtained from the model with experimental observations and prevailing views on crowding inside cells.

2.5. Our Model and Experimental Data. There is now a growing consensus that crowded spaces such as cell cytoplasm cannot be regarded as a mixed bag of proteins where excluded volume effects alone dominate.[43] A polymeric crowding sensor based on fluorescence resonance energy transfer revealed no compression inside the cell, suggesting minimal role for excluded volume effects.[44] Weak "quinary" interactions between a macromolecule and its surroundings can create spatial networks of macromolecules that can define functional regions in cells.[45,46] The view that metabolic reactions in cytoplasm or mitochondrial matrix are carried out in enzyme complexes clustered together by quinary interactions (metabolon)[47,48] and driven by substrate channeling[49−51] is gaining acceptance. Indeed, a randomly scattered set of enzymes in a metabolic pathway will experience slowed reaction rates,[52] owing to diminished presence of metabolic intermediates at the active site, random diffusion of substrates, and nonspecific interactions of the substrate with surrounding crowder macromolecules as revealed by the proposed residence time MC model. Our model underscores the enormous entropic advantage accrued by sequential ordering of enzymes.

Measurement of experimental residence times of small molecules inside living cells is currently a challenging task. Residence time of rRNA transcription termination factor mTTF-1 tagged with EGFP in the nucleus of HeLa cells was measured to be 13 s.[53] In absence of such data, the presented model predicts that even in the midst of moderate levels of crowding, (a_f = 0.1−0.2), increased nonspecific association of the substrate can seriously impede its diffusion, leading to steep drop in enzyme reaction rates.

2.5.1. Model Explaining Alkaline Phosphatase Hydrolysis Results (Q. 2.2a). The results shown in Figure 2a are qualitatively similar to the decrease observed in the reaction rate (Figure 4a (inset)) and diffusivity, D (Figure 5a), with increasing area fractions of the point obstacle. In Figure 2b, the size of dextran can be assumed to scale with the residence time used in the model. Dextran is a flexible ribbon-like polymer.[54] A higher molecular weight of dextran is likely to offer a larger surface area, which can bind/trap the substrate (PNPP) for sufficiently longer residence and relaxation times. Thus, it is evident that influence of residence time on the reaction rate predominates over excluded volume effects when size of the crowding obstacle is large (∼2000 kDa) or when volume fraction of a moderately sized crowding agent (∼500 kDa dextran) is high (>15% w/w). The above result is qualitatively similar to the decrease observed in the reaction rate [Figure 4b (inset)] and diffusivity, D (Figure 5b), with increasing residence times of point obstacles. The trend observed with reciprocal relaxation time (Figure 6) also mirrors the results shown in Figure 2. Thus, increased stickiness of the crowder can profoundly diminish substrate diffusion and consequently the enzymatic reaction rate. This is in agreement with previous experimental results where larger molecular weight dextrans slowed the rate of alkaline phosphatase-catalyzed hydrolysis of *p*-nitrophenyl phosphate noticeably more than smaller dextrans.[31]

For a quantitative comparison of the results from the model with experimental results in Figure 2, a 3D model is necessary with further refinements such as: (i) modifying the interaction between the obstacle and substrate in terms of one or more intermediate steps; and (ii) a distribution of residence times to match the complexity of the intracellular milieu.

2.5.2. Model Explaining Pastor and Co-Worker's Results (Q. 2.2b). Our results explain why effects of crowding by large obstacles are more pronounced with enzymes of larger size compared to smaller size. The ratio of enzyme active site area to its total exposed surface area decreases rapidly as enzyme size increases. This makes the search for the active site in the larger enzyme more tortuous for the diffusing substrate. For identical amounts of excluded volume, the presence of small crowders will hold back the substrate for shorter residence times in comparison to larger crowders (which have higher surface area to trap the substrate), implying that when enzymes are small, reaction velocity is predominantly affected by excluded volume.[45] Thus, larger crowders exacerbate the slow reaction rate in larger enzymes by increasing residence time of the substrate that already has a tortuous path to navigate to find the target active site.

The results from our numerical model involving a single enzyme, surplus single substrate, and numerous point obstacles clearly establish the role of volume exclusion and residence time in slowing down the enzymatic reaction rate.

2.5.3. Q.2.2c. Free glycolytic metabolites are scarce to find in rat/rabbit muscle because they are more likely to be nonspecifically bound to crowding macromolecules in the muscle interior.

2.5.4. Q.2.2d. Diffusion coefficient of ATP is likely to be slowed inside skeletal muscle/cardiomyocytes for chiefly two reasons: (i) increased fluid viscosity that it experiences and (ii) frequent collisions and nonspecific interactions of ATP with surrounding macromolecules, which can increase the residence time of bound ATP.

2.5.5. Model Explaining Other Data in Literature. There have been numerous studies on the influence of crowding agents such as dextrans,[31,55,56] Ficolls,[31,36] proteins,[56,57] or poly(ethylene glycol)[37] on enzyme kinetics in vitro. However, only a few studies have accounted for the role of nonspecific binding presumably because either such binding is hard to measure experimentally or the size of the crowders employed were much less than 2000 kDa making such binding irrelevant. Wenner and Bloomfeld found increased nonspecific binding of substrate/product to Ficoll 70 during EcoRV-catalyzed cleavage of DNA. However, they observed that reaction velocity was nearly unaffected presumably because of the small size (70 kDa) and compact nature of Ficolls compared to dextrans.[36] Interestingly, work by Poggi and Slade suggests that nature of the crowder (neutral vs charged) can also play a role in influencing the enzyme kinetic parameters.[56] They observed increased V_{max} for anionic substrates in the presence of highly charged crowders such as hen lysozyme in contrast to neutral crowders such as dextrans. Perhaps reduced nonspecific binding of the substrate with lysozyme owing to electrostatic repulsions may have contributed to increased enzymatic activity in comparison to dextrans. Often crowding effects can be complicated by oligomerization of the enzyme which may enhance or diminish the activity.[57] Recently, Zotter et al. measured enzymatic activity of TEM1 β-lactamase inside living HeLa cells. They observed a reduced catalytic efficiency for the enzyme in vivo compared to in vitro.[58] The reduced activity of

DOI: 10.1021/acsomega.8b02863
ACS Omega 2019, 4, 727−736

the enzyme was chiefly attributed to attenuated diffusion of the substrate inside the cell owing to interactions with cell components. Their results clearly suggest that the amount of free substrate in the cell interior is significantly lower than the total substrate, consistent with our arguments here. These data reinforce further the role of sticky substrate as an enzymatic rate-limiting factor inside the living cell and make our model pertinent.

The enzymatic reaction considered here is completely diffusion limited, and the results obtained are explainable in terms of diffusion in disordered systems. It is therefore intriguing to note that such a simple model of enzymatic reaction based on diffusion and percolation phenomena only is able to explain qualitatively the experimental observations highlighted above.

3. CONCLUSIONS

A novel residence time MC model is proposed to account for the myriad interactions encountered by a diffusing substrate in crowded physiological spaces before it reaches the target enzyme active site. The enzyme reaction dynamics was investigated using parameters such as enzymatic reaction rate, product diffusivity, and relaxation time of substrate/product. It is shown that enhanced nonspecific binding/trapping of the substrate by the crowder dramatically diminishes the enzymatic reaction rate. The kinetic trends observed in the model with increasing residence time of the substrate were in qualitative agreement with experimental enzyme kinetics data obtained in aqueous media using alkaline phosphatase and crowding dextran macromolecules in a range of sizes. Such a result implies that free diffusion of the substrate or reaction intermediates in a metabolic pathway can severely compromise the final product yield in the pathway. The role of clustered enzymes held together by weak quinary interactions while channeling the reaction intermediates for meeting urgent metabolic demands appears to be a natural way to safeguard against free diffusion of the substrate. The results from the proposed model thus provide crucial insights justifying the need for the presence of the metabolon.

4. EXPERIMENTAL SECTION

Alkaline phosphatase (bovine intestinal mucosa) and dextrans (*Leuconostoc mesenteriodes*) of molecular weights 40, 500, and 2000 kDa were purchased from Sigma-Aldrich Chemicals Pvt. Ltd., India. The polydispersities of the dextrans were typically less than 2.0 as reported by the manufacturer. Glycine and Na_2HPO_4 of analytical grade were obtained from MERCK, whereas *p*-nitrophenyl phosphate disodium salt was bought from Sisco Research Laboratories, India. All other chemicals employed were of analytical grade.

4.1. Hydrolysis of PNPP by Alkaline Phosphatase. A typical reaction mixture contained alkaline phosphatase (2 μM) and PNPP dissolved in an aqueous solution of 100 mM glycine buffered at pH 9.5. The PNPP concentration was kept at 1 mM, which is well above the measured K_m under the reaction conditions employed (0.25 mM). The concentration of dextran in the medium was varied between 0 and 30% (w/w). For larger dextrans, such as 2000 kDa, kinetic measurements with higher concentrations such as 25 or 30% w/w were not possible due to problems related to solubility and mixing. The total weight of the reaction medium was kept constant at 1.0 g. All samples were made in deionized water. Crowding agents increase bulk viscosity of samples. Thus, the reaction was initiated by forcefully mixing the enzyme (typically ~50 μL in buffered aqueous medium) with an aqueous buffered mixture containing the substrate and crowding agent (typically ~950 μL) in an Eppendorf tube using a syringe. This mixture was vigorously agitated in a vortex mixer for 30 s. Immediately after, the mixture was transferred to a cuvette, and the progress of the reaction was conveniently monitored by recording the absorbance of the product *p*-nitrophenol at 450 nm after a dead time of 30 s using a double beam spectrophotometer (CARY 100, Varian, USA). All samples were run in duplicates. All experiments were done at room temperature (298 K).

4.2. Calculation of Rate of Reaction. The initial velocity, *V*, was obtained from the slope (linear regression) of the first 20 s of the recorded absorbance/time data. The initial velocity observed under identical conditions, but in the complete absence of the crowding species, was referred to as V_0. This was normalized to a value of 100 for ease in comparison of velocities obtained in presence of crowding. The points depicted (Figure 2) are the averages of at least three independent experiments done on different days. Blank solutions containing a mixture of the crowding agent (25% w/w) employed and the corresponding substrate showed negligible change in the absorbance in the complete absence of the enzyme under identical conditions.

AUTHOR INFORMATION

Corresponding Author

*E-mail: rsw@iitg.ac.in.

ORCID

Rajaram Swaminathan: 0000-0003-1294-8379

Present Addresses

§Predomix Technologies Private Limited, E-2226 Palam Vihar, Gurgaon 122017, Haryana, India.

∥563 E McKinley Ave, Unit B, Sunnyvale CA 94086, United States of America.

⊥Molecular Modelling and Simulation Laboratory, Department of Molecular Biology and Biotechnology, Tezpur University, Tezpur 784 028, Assam, India.

Notes

The authors declare no competing financial interest.

ACKNOWLEDGMENTS

The authors express their gratitude to IIT Guwahati for providing the computational and experimental facilities that made this work possible. R.S. wishes to thank Dr. Gautam I. Menon at the Institute of Mathematical Sciences, Chennai for the several discussions they had together.

REFERENCES

(1) Fulton, A. B. How crowded is the cytoplasm? *Cell* **1982**, *30*, 345−347.

(2) Luby-Phelps, K. The physical chemistry of cytoplasm and its influence on cell function: an update. *Mol. Biol. Cell* **2013**, *24*, 2593−2596.

(3) Zimmerman, S. B.; Trach, S. O. Estimation of macromolecule concentrations and excluded volume effects for the cytoplasm of Escherichia coli. *J. Mol. Biol.* **1991**, *222*, 599−620.

(4) Goodsell, D. S. Inside a living cell. *Trends Biochem. Sci.* **1991**, *16*, 203−206.

(5) Partikian, A.; Ölveczky, B.; Swaminathan, R.; Li, Y.; Verkman, A. S. Rapid diffusion of green fluorescent protein in the mitochondrial matrix. *J. Cell Biol.* **1998**, *140*, 821−829.

DOI: 10.1021/acsomega.8b02863
ACS Omega 2019, 4, 727−736

(6) Dieteren, C. E. J.; Gielen, S. C. A. M.; Nijtmans, L. G. J.; Smeitink, J. A. M.; Swarts, H. G.; Brock, R.; Willems, P. H. G. M.; Koopman, W. J. H. Solute diffusion is hindered in the mitochondrial matrix. *Proc. Natl. Acad. Sci. U.S.A.* **2011**, *108*, 8657−8662.
(7) Doster, W.; Longeville, S. Microscopic diffusion and hydrodynamic interactions of hemoglobin in red blood cells. *Biophys. J.* **2007**, *93*, 1360−1368.
(8) Spitzer, J. From water and ions to crowded biomacromolecules: In vivo structuring of a prokaryotic cell. *Microbiol. Mol. Biol. Rev.* **2011**, *75*, 491−506.
(9) Berry, H. Monte Carlo simulations of enzyme reactions in two dimensions: Fractal kinetics and spatial segregation. *Biophys. J.* **2002**, *83*, 1891−1901.
(10) Schnell, S.; Turner, T. E. Reaction kinetics in intracellular environments with macromolecular crowding: Simulations and rate laws. *Prog. Biophys. Mol. Biol.* **2004**, *85*, 235−260.
(11) Grima, R.; Schnell, S. How reaction kinetics with time-dependent rate coefficients differs from generalized mass action. *ChemPhysChem* **2006**, *7*, 1422−1424.
(12) Kao, H. P.; Abney, J. R.; Verkman, A. S. Determinants of the translational mobility of a small solute in cell cytoplasm. *J. Cell Biol.* **1993**, *120*, 175−184.
(13) Swaminathan, R.; Hoang, C. P.; Verkman, A. S. Photobleaching recovery and anisotropy decay of green fluorescent protein GFP-S65T in solution and cells: Cytoplasmic viscosity probed by green fluorescent protein translational and rotational diffusion. *Biophys. J.* **1997**, *72*, 1900−1907.
(14) Seksek, O.; Biwersi, J.; Verkman, A. S. Translational diffusion of macromolecule-sized solutes in cytoplasm and nucleus. *J. Cell Biol.* **1997**, *138*, 131−142.
(15) Sims, J. K.; Manteiga, S.; Lee, K. Towards high resolution analysis of metabolic flux in cells and tissues. *Curr. Opin. Biotechnol.* **2013**, *24*, 933−939.
(16) Hou, B.-H.; Takanaga, H.; Grossmann, G.; Chen, L.-Q.; Qu, X.-Q.; Jones, A. M.; Lalonde, S.; Schweissgut, O.; Wiechert, W.; Frommer, W. B. Optical sensors for monitoring dynamic changes of intracellular metabolite levels in mammalian cells. *Nat. Protoc.* **2011**, *6*, 1818−1833.
(17) Jones, A. M.; Grossmann, G.; Danielson, J. T.; Sosso, D.; Chen, L.-Q.; Ho, C.-H.; Frommer, W. B. In vivo biochemistry: Applications for small molecule biosensors in plant biology. *Curr. Opin. Plant Biol.* **2013**, *16*, 389−395.
(18) Merrins, M. J.; Van Dyke, A. R.; Mapp, A. K.; Rizzo, M. A.; Satin, L. S. Direct Measurements of Oscillatory Glycolysis in Pancreatic Islet β-Cells Using Novel Fluorescence Resonance Energy Transfer (FRET) Biosensors for Pyruvate Kinase M2 Activity. *J. Biol. Chem.* **2013**, *288*, 33312−33322.
(19) Fehr, M.; Lalonde, S.; Ehrhardt, D. W.; Frommer, W. B. Live imaging of glucose homeostasis in nuclei of COS-7 cells. *J. Fluoresc.* **2004**, *14*, 603−609.
(20) Albe, K. R.; Butler, M. H.; Wright, B. E. Cellular concentrations of enzymes and their substrates. *J. Theor. Biol.* **1990**, *143*, 163−195.
(21) Hubley, M. J.; Moerland, T. S.; Rosanske, R. C. Diffusion coefficients of ATP and creatine phosphate in isolated muscle: pulsed gradient ^{31}P NMR of small biological samples. *NMR Biomed.* **1995**, *8*, 72−78.
(22) Vendelin, M.; Birkedal, R. Anisotropic diffusion of fluorescently labeled ATP in rat cardiomyocytes determined by raster image correlation spectroscopy. *Am. J. Physiol.: Cell Physiol.* **2008**, *295*, C1302−C1315.
(23) Suzuki, K.; Sheetz, M. P. Binding of cross-linked glycosylphosphatidylinositol-anchored proteins to discrete actin-associated sites and cholesterol-dependent domains. *Biophys. J.* **2001**, *81*, 2181−2189.
(24) Vértessy, B. G.; Orosz, F.; Kovács, J.; Ovádi, J. Alternative Binding of Two Sequential Glycolytic Enzymes to Microtubules. *J. Biol. Chem.* **1997**, *272*, 25542−25546.
(25) Nelson, D. L.; Cox, M. M. *Lehninger Principles of Biochemistry*; W. H. Freeman, 2012.
(26) Mourão, M.; Kreitman, D.; Schnell, S. Unravelling the impact of obstacles in diffusion and kinetics of an enzyme catalysed reaction. *Phys. Chem. Chem. Phys.* **2014**, *16*, 4492−4503.
(27) Vilaseca, E.; Isvoran, A.; Madurga, S.; Pastor, I.; Garcés, J. L.; Mas, F. New insights into diffusion in 3D crowded media by Monte Carlo simulations: effect of size, mobility and spatial distribution of obstacles. *Phys. Chem. Chem. Phys.* **2011**, *13*, 7396−7407.
(28) Nałęcz-Jawecki, P.; Szymańska, P.; Kochańczyk, M.; Miękisz, J.; Lipniacki, T. Effective reaction rates for diffusion-limited reaction cycles. *J. Chem. Phys.* **2015**, *143*, 215102.
(29) Agrawal, M.; Santra, S. B.; Anand, R.; Swaminathan, R. Effect of macromolecular crowding on the rate of diffusion-limited enzymatic reaction. *Pramana—J. Phys.* **2008**, *71*, 359−368.
(30) Pitulice, L.; Vilaseca, E.; Pastor, I.; Madurga, S.; Garcés, J. L.; Isvoran, A.; Mas, F. Monte Carlo simulations of enzymatic reactions in crowded media. Effect of the enzyme-obstacle relative size. *Math. Biosci.* **2014**, *251*, 72−82.
(31) Homchaudhuri, L.; Sarma, N.; Swaminathan, R. Effect of crowding by dextrans and ficolls on the rate of alkaline phosphatase-catalyzed hydrolysis: A size-dependent investigation. *Biopolymers* **2006**, *83*, 477−486.
(32) Pastor, I.; Pitulice, L.; Balcells, C.; Vilaseca, E.; Madurga, S.; Isvoran, A.; Cascante, M.; Mas, F. Effect of crowding by Dextrans in enzymatic reactions. *Biophys. Chem.* **2014**, *185*, 8−13.
(33) Stauffer, D.; Aharony, A. *Introduction to Percolation Theory*; Taylor and Francis: London, 1994.
(34) Le Doussal, P.; Monthus, C. Reaction diffusion models in one dimension with disorder. *Phys. Rev. E: Stat. Phys., Plasmas, Fluids, Relat. Interdiscip. Top.* **1999**, *60*, 1212−1238.
(35) Laurent, T. C. Enzyme reactions in polymer media. *Eur. J. Biochem.* **1971**, *21*, 498−506.
(36) Wenner, J. R.; Bloomfield, V. A. Crowding Effects on Eco RV Kinetics and Binding. *Biophys. J.* **1999**, *77*, 3234−3241.
(37) Asaad, N.; Engberts, J. B. F. N. Cytosol-Mimetic Chemistry: Kinetics of the Trypsin-Catalyzed Hydrolysis of p-Nitrophenyl Acetate upon Addition of Polyethylene Glycol and N-tert-Butyl Acetoacetamide. *J. Am. Chem. Soc.* **2003**, *125*, 6874−6875.
(38) Ellis, R. J. Macromolecular crowding: Obvious but underappreciated. *Trends Biochem. Sci.* **2001**, *26*, 597−604.
(39) Havlin, S.; Ben-Avraham, D. DIFFUSION IN DISORDERED MEDIA. *Adv. Phys.* **1987**, *36*, 695−798.
(40) Santra, S. B.; Seitz, W. A. Diffusion under crossed local and global biases in disordered systems. *Int. J. Mod. Phys. C* **2000**, *11*, 1357−1369.
(41) Saxton, M. J. Anomalous diffusion due to obstacles: A Monte Carlo study. *Biophys. J.* **1994**, *66*, 394−401.
(42) Putzel, G. G.; Tagliazucchi, M.; Szleifer, I. Nonmonotonic diffusion of particles among larger attractive crowding spheres. *Phys. Rev. Lett.* **2014**, *113*, 138302.
(43) Politou, A.; Temussi, P. A. Revisiting a dogma: The effect of volume exclusion in molecular crowding. *Curr. Opin. Struct. Biol.* **2015**, *30*, 1−6.
(44) Gnutt, D.; Gao, M.; Brylski, O.; Heyden, M.; Ebbinghaus, S. Excluded-volume effects in living cells. *Angew. Chem., Int. Ed.* **2015**, *54*, 2548−2551.
(45) Aon, M. A.; Cortassa, S. Function of metabolic and organelle networks in crowded and organized media. *Front. Physiol.* **2015**, *5*, 523.
(46) Chien, P.; Gierasch, L. M. Challenges and dreams: Physics of weak interactions essential to life. *Mol. Biol. Cell* **2014**, *25*, 3474−3477.
(47) Wu, F.; Pelster, L. N.; Minteer, S. D. Krebs cycle metabolon formation: Metabolite concentration gradient enhanced compartmentation of sequential enzymes. *Chem. Commun.* **2015**, *51*, 1244−1247.
(48) Wirth, A. J.; Gruebele, M. Quinary protein structure and the consequences of crowding in living cells: Leaving the test-tube behind. *BioEssays* **2013**, *35*, 984−993.
(49) Bulutoglu, B.; Garcia, K. E.; Wu, F.; Minteer, S. D.; Banta, S. Direct Evidence for Metabolon Formation and Substrate Channeling

DOI: 10.1021/acsomega.8b02863
ACS Omega 2019, 4, 727−736

in Recombinant TCA Cycle Enzymes. *ACS Chem. Biol.* **2016**, *11*, 2847−2853.
(50) Wheeldon, I.; Minteer, S. D.; Banta, S.; Barton, S. C.; Atanassov, P.; Sigman, M. Substrate channelling as an approach to cascade reactions. *Nat. Chem.* **2016**, *8*, 299−309.
(51) Mao, Q.; Schunk, T.; Gerber, B.; Erni, B. A String of Enzymes, Purification and Characterization of a Fusion Protein Comprising the Four Subunits of the Glucose Phosphotransferase System of *Escherichia coli*. *J. Biol. Chem.* **1995**, *270*, 18295−18300.
(52) Anderson, J. B.; Anderson, L. E.; Kussmann, J. Monte Carlo simulations of single- and multistep enzyme-catalyzed reaction sequences: Effects of diffusion, cell size, enzyme fluctuations, colocalization, and segregation. *J. Chem. Phys.* **2010**, *133*, 034104.
(53) Wachsmuth, M.; Weidemann, T.; Müller, G.; Hoffmann-Rohrer, U. W.; Knoch, T. A.; Waldeck, W.; Langowski, J. Analyzing intracellular binding and diffusion with continuous fluorescence photobleaching. *Biophys. J.* **2003**, *84*, 3353−3363.
(54) Venturoli, D.; Rippe, B. Ficoll and dextran vs. globular proteins as probes for testing glomerular permselectivity: Effects of molecular size, shape, charge, and deformability. *Am. J. Physiol. Renal. Physiol.* **2005**, *288*, F605−F613.
(55) Schneider, S. H.; Lockwood, S. P.; Hargreaves, D. I.; Slade, D. J.; LoConte, M. A.; Logan, B. E.; McLaughlin, E. E.; Conroy, M. J.; Slade, K. M. Slowed Diffusion and Excluded Volume Both Contribute to the Effects of Macromolecular Crowding on Alcohol Dehydrogenase Steady-State Kinetics. *Biochemistry* **2015**, *54*, 5898−5906.
(56) Poggi, C. G.; Slade, K. M. Macromolecular crowding and the steady-state kinetics of malate dehydrogenase. *Biochemistry* **2015**, *54*, 260−267.
(57) Minton, A. P.; Wilf, J. Effect of macromolecular crowding upon the structure and function of an enzyme: Glyceraldehyde-3-phosphate dehydrogenase. *Biochemistry* **1981**, *20*, 4821−4826.
(58) Zotter, A.; Bäuerle, F.; Dey, D.; Kiss, V.; Schreiber, G. Quantifying enzyme activity in living cells. *J. Biol. Chem.* **2017**, *292*, 15838−15848.

DOI: 10.1021/acsomega.8b02863
ACS Omega 2019, 4, 727−736